IEICE TRANS. COMMUN., VOL.E91–B, NO.7 JULY 2008

PAPER

On Cellular MIMO Channel Capacity

Koichi ADACHI[†a)], ***Student Member***, **Fumiyuki ADACHI**[††], ***and*** **Masao NAKAGAWA**[†], ***Fellows***

SUMMARY To increase the transmission rate without bandwidth expansion, the multiple-input multiple-output (MIMO) technique has recently been attracting much attention. The MIMO channel capacity in a cellular system is affected by the interference from neighboring co-channel cells. In this paper, we introduce the cellular channel capacity and evaluate its outage capacity, taking into account the frequency-reuse factor, path loss exponent, standard deviation of shadowing loss, and transmission power of a base station (BS). Furthermore, we compare the cellular MIMO downlink channel capacity with those of other multi-antenna transmission techniques such as single-input multiple-output (SIMO) and space-time block coded multiple-input single-output (STBC-MISO). We show that the optimum frequency-reuse factor F that maximizes 10%-outage capacity is 3 and both 50%- and 90%-outage capacities is 1 irrespective of the type of multi-antenna transmission technique, where q%-outage capacity is defined as the channel capacity that gives an outage probability of q%. We also show that the cellular MIMO channel capacity is always higher than those of SIMO and STBC-MISO.

key words: *MIMO, multi-cell environemnt, channel capacity*

1. Introduction

Multiple-input multiple-output (MIMO) transmission is known as a promising technique to increase the transmission rate without bandwidth expansion [1]. In the cellular system, the same carrier frequency is reused at different cells to efficiently utilize the limited bandwidth. Therefore, the channel capacity is affected by not only the noise but also the co-channel interference (CCI) from the neighboring co-channel cells. The channel capacity can be increased using the MIMO technique by a factor of the number of transmit antennas but is degraded by CCI. To mitigate the adverse effect of CCI, it is necessary to increase the distance between the cells using the same carrier frequency (i.e., to increase the frequency-reuse factor). But, this reduces the channel capacity per cell. This is because as the frequency-reuse factor increases, the bandwidth allocated to each cell is made narrower.

In [2] and [3], the channel capacity improvement by MIMO technique over the single-input single-output (SISO) technique and single-input multiple-output (SIMO) technique in a cellular environment is evaluated by taking into account the propagation parameters and transmit power. However, the impact of frequency-reuse factor on the channel capacity per cell with MIMO technique has not yet been fully investigated. It is practically important to see if the MIMO technique can increase the channel capacity per cell. In [4], MIMO with singular value decomposition (SVD) is considered and the impact of cell-sectorization and frequency-reuse factor on the user peak throughput and median channel capacity per cell is evaluated to show that the universal frequency-reuse (or the single frequency-reuse) provides the highest capacity. The throughput improvement of MIMO with SVD over SIMO is discussed in [5]. Since Alamouti proposed the space-time block codes (STBC) [6], the multiple-input single-output (MISO) downlink transmit diversity [7] has been attracting much attention because the complexity problem of a mobile terminal can be alleviated. To the best of authors' knowledge, the comprehensive capacity comparison of SISO, SIMO, STBC-MISO, and MIMO in a cellular system is not available in any literature. So far, no literature discussed about the cellular MIMO channel capacity when the capacity enhancement technique (such as power allocation based on the water filling theory) is used. Furthermore, the impact of propagation parameters (e.g., path loss exponent and shadowing loss standard deviation) on the cellular MIMO channel capacity is also not available in any literature.

The channel capacity varies according to the distance-dependent path loss, shadowing loss and multipath fading. In this paper, we call the channel capacity per cell as the cellular channel capacity. Recently published papers [2], [3] focus on the mean spectral efficiency, which is the cellular channel capacity averaged over positions of users uniformly distributed in the cell. The cellular channel capacity is a random variable and therefore, the theoretical analysis of cellular channel capacity is quite difficult if not impossible. In this paper, we first obtain the information outage probability for the given frequency-reuse factor and then, find the q%-outage capacity [8], [9] (which is defined as the channel capacity that gives an outage probability of q%). We consider the 10%-, 50%-, and 90%-outage capacities and discuss the optimum frequency-reuse factor F that maximizes the each outage capacity using MIMO technique (cellular MIMO channel capacity).

The rest of the paper is organized as follows. In Sect. 2, the system model is described and the cellular channel capacity formula is presented. Simulation setup is given and then numerical results of information outage capacity and

Manuscript received September 26, 2007.
Manuscript revised March 1, 2008.

[†]The authors are with School of Science for Open and Environmental Systems, Graduate School of Science and Technology, Keio University, Yokohama-shi, 223-8522 Japan.
[††]The author is with the Department of Electrical and Communication Engineering, Graduate School of Engineering, Tohoku University, Sendai-shi, 980-8579 Japan.
a) E-mail: kouichi@nkgw.ics.keio.ac.jp

DOI: 10.1093/ietcom/e91–b.7.2366

$q\%$-outage capacity are presented in Sect. 3. Section 4 concludes the paper.

2. Cellular System and Cellular Channel Capacity

In this paper, the hexagonal cell layout is considered as shown in Fig. 1. The center cell is a cell of interest. The same frequency is reused at different cells with the frequency-reuse factor F $(= i^2 + j^2 + ij = 1, 3, 4, 7, 9, 12\cdots,$ i and j are a positive integer) [10] as shown in Fig. 2 for the case of $F = 3$. We assume a MIMO system with N_t transmit antennas and N_r receive antennas. The base station (BS) is located in the center of its cell. No sector antenna is used at the BS.

A mobile station (MS) of interest receives the CCI from the c-th cell ($c = 1, 2\cdots$) as well as the desired signal from its communicating cell indexed by $c = 0$. The local average received power $P_{r,c}$ (averaged over the fading statistics only), on each receive antenna, of the c-th BS can be expressed as

$$P_{r,c} = A \cdot P_t \cdot d_c^{-\alpha} \cdot 10^{-\xi_c/10} \tag{1}$$

where A is a constant value (depending on the antenna gain, feeder loss, etc), P_t is the total transmit power from each BS, d_c is the distance between the c-th BS and the MS communicating with the $c = $ 0th BS, α is the path loss exponent, and ξ_c is the shadowing loss in dB following a zero-mean Gaussian distribution with the standard deviation σ. If either STBC-MISO or MIMO is used, the transmit power from each antenna is reduced by a factor of N_t to keep the total transmit power from a BS the same.

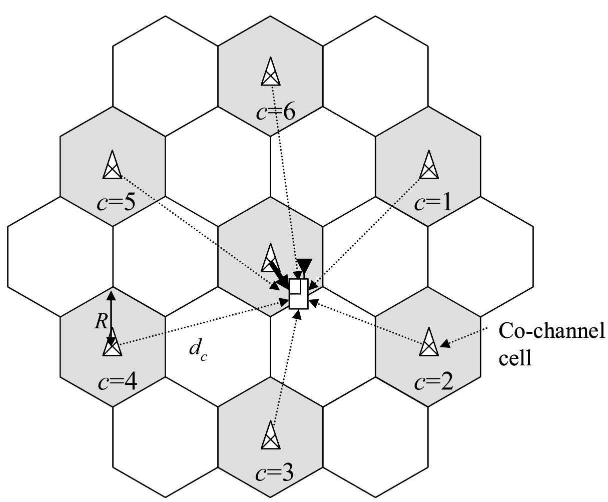

Fig. 1 Cell layout ($F = 3$).

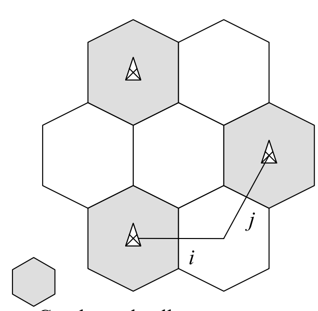

Fig. 2 Geographical relationship between the $c = $ 0th cell and co-channnel cells ($F = 3$).

Equation (1) is rewritten as

$$P_{r,c} = S \cdot r_c^{-\alpha} \cdot 10^{-\xi_c/10} \tag{2}$$

where $r_c = d_c/R$ is the normalized distance with R being the cell radius and $S = A \cdot P_t \cdot R^{-\alpha}$ is the average signal power received by an MS at the cell edge ($d_0 = R$). The total local average CCI power I from the co-channel cells is expressed as

$$I = \sum_{c=1}^{\infty} S \cdot r_c^{-\alpha} \cdot 10^{-\xi_c/10} \tag{3}$$

In this paper, the CCI is approximated as a zero-mean complex Gaussian process with the average power I. The noise power N due to the additive white Gaussian noise (AWGN) is given as

$$N = N_0 \cdot W \tag{4}$$

where N_0 is the one-sided power spectrum density of the AWGN and W is the channel bandwidth assigned to each cell.

The local average received signal-to-interference plus noise power ratio (SINR) γ on each receive antenna is given as

$$\gamma = \frac{P_{r,0}}{I + N} = \frac{r_0^{-\alpha} \cdot 10^{-\xi_0/10}}{\sum_{c=1}^{\infty} r_c^{-\alpha} \cdot 10^{-\xi_c/10} + \left(\frac{E_s}{N_0}\right)^{-1}} \tag{5}$$

where E_s/N_0 $(= (S/W)/N_0)$ denotes the average signal energy per data symbol-to-AWGN power spectrum density ratio at the cell edge.

Since the total system bandwidth required for a cellular system with the frequency-reuse factor F is $B = F \cdot W$ (Hz). The cellular MIMO channel capacity is defined as the channel capacity per cell C normalized by the system bandwidth B and is given by

$$\eta = \frac{1}{F} \cdot \frac{C}{W} \tag{6}$$

where C/W (bps/Hz) is given by [1]

$$\frac{C}{W} = \log_2 \det\left[\mathbf{I}_{N_r} + \frac{\gamma}{N_t} \cdot \mathbf{H}\mathbf{H}^H\right] \tag{7}$$

In the above, $\mathbf{I}_{N_r}$ is the $N_r \times N_r$ identity matrix, $\mathbf{H}$ is the $N_r \times N_t$ channel matrix between the $c = $ 0th BS and the MS of interest and is expressed as

$$\mathbf{H} = \begin{pmatrix} h_{0,0} & & h_{0,N_t-1} \\ & \ddots & \\ h_{N_r-1,0} & & h_{N_r-1,N_t-1} \end{pmatrix} \tag{8}$$

Table 1 Coding rate R_c of STBC-MISO [11].

Number of transmit antennas	Coding rate R_c
2	1
3	3/4
4	
5	2/3
6	

where h_{n_r,n_t} is the complex channel gain with $E\left[\left|h_{n_r,n_t}\right|^2\right] = 1$, due to multipath fading, between the n_t-th transmit antenna of the $c = 0$th BS and the n_r-th receive antenna of the MS ($E[.]$ denotes the ensemble average operation). By substituting Eq. (7) into Eq. (6), we have the following cellular channel capacity η (bps/Hz/cell)

$$\eta = \frac{1}{F} \cdot \frac{C}{W} = \frac{1}{F} \cdot \log_2 \det\left[\mathbf{I}_{N_r} + \frac{\gamma}{N_t} \cdot \mathbf{H}\mathbf{H}^H\right] \tag{9}$$

The cellular channel capacity of SISO, SIMO and STBC-MISO can be obtained, similar to the MIMO case, as

$$\eta = \begin{cases} \dfrac{1}{F} \cdot \log_2\left[1 + \gamma \cdot \left|h_{0,0}\right|^2\right] & \text{for SISO} \\ \dfrac{R_c}{F} \cdot \log_2\left[1 + \dfrac{\gamma}{N_t} \cdot \sum\limits_{n_t=0}^{N_t-1} \left|h_{0,n_t}\right|^2\right] & \text{for STBC} - \text{MISO} \\ \dfrac{1}{F} \cdot \log_2\left[1 + \gamma \cdot \sum\limits_{n_r=0}^{N_r-1} \left|h_{n_r,0}\right|^2\right] & \text{for SIMO} \end{cases} \tag{10}$$

where R_c is the coding rate of STBC-MISO shown in Table 1 [11].

As the frequency-reuse factor F increases, the CCI power I from co-channel cells becomes weaker (this increases the cellular channel capacity), while the total bandwidth $F \cdot W$ necessary for a cellular system increases (this reduces the cellular channel capacity). This suggests that there may be an optimum F that maximizes the cellular channel capacity η. However, the value of η is a random variable due to the distance-dependent path loss, shadowing loss and multipath fading. Using the Monte-Carlo numerical evaluation, we find the outage capacity defined as the capacity of η falling below a certain value.

3. Numerical Results

We consider 1×1 SISO, 1×4 SIMO, 4×1 STBC-MISO, and 4×4 MIMO except for Fig. 8. Note that when 4×1 STBC-MISO is used, the coding rate reduces to 3/4 [7]. Table 2 summarizes the numerical condition. The location of MS is uniformly distributed within the center cell. We assume an uncorrelated frequency-nonselective block Rayleigh fading channel for each transmit antenna/receive antenna pair. In the Monte-Carlo numerical evaluation, each Rayleigh fading is generated based on modified Jakes' model [12]. The total transmit power of each cell is determined so that the received SINR at the cell edge becomes the predetermined value $\Gamma(= E_s/N_0) = 0 \sim 20$ dB.

Table 2 Numerical condition.

Cell structure		Hexagonal
Frequency-reuse factor		$F = 1, 3, 4, 7, 9, 12$
MS distribution		Uniform
Path loss exponent		$\alpha = 3.0$–4.0
Shadowing standard deviation		$\sigma = 4.0$–8.0 dB
Channel model	Multipath fading	Block Rayleigh fading
	Number of paths	1
	Max. Doppler frequency	$f_D \to 0$ Hz
Number of transmit antennas		$N_t = 1$–6
Number of receive antennas		$N_r = 1$–6

The distribution of the cellular channel capacity is found as follows. The location of MS of interest is randomly generated in the center cell ($c = 0$th cell). The path loss and shadowing loss between each co-channel cell and MS are generated and the received SINR, γ, is computed using Eq. (5) and then, the cellular channel capacity is computed using Eq. (9) or (10). The distribution of the cellular channel capacity is obtained for the given frequency-reuse factor F by repeating the above process a sufficient number of times. In the Monte-Carlo numerical evaluation, the number of co-channel interfering cells is set to be 18 for $F = 1$ and 6 for $F \neq 1$ because interference from other cells can be neglected. The shadowing loss is modeled as the log-normally distributed random variable having the standard deviation σ dB and those experienced at different BSs are assumed to be independent. The MS of interest is always connected to the $c = 0$th cell irrespective of the received signal power from other BSs.

3.1 Information Outage Probability

To find the q%-outage capacity we first obtain the information outage probability of multi-antenna technique. The information outage probabilities of 1 × 1 SISO, 1 × 4 SIMO, 4 × 1 STBC-MISO, and 4 × 4 MIMO are plotted in Fig. 3. Since the transmit power from each antenna is reduced by a factor of N_t to keep the total transmit power P_t from each BS the same, the received SINR at the MS is reduced when multiple transmit antennas are used at BS, thereby increasing the probability that the cellular channel capacity drops. However, the transmission data rate of 4 × 4 MIMO is four times higher than that of 1 × 4 SIMO and hence, the cellular MIMO channel capacity becomes higher than 1×4 SIMO. It can be seen from the figures that as F increases, the capacity improvement of the MIMO over the SIMO becomes larger. The reason for this can be explained as follows. In a low SINR region, the spatial diversity gain is more important than the spatial multiplexing gain and therefore, the superiority of MIMO over SIMO diminishes. On the other hand, in a high SINR region, the spatial multiplexing gain is more effective than the spatial diversity gain and hence, MIMO provides larger capacity than SIMO. As F increases, the interference gets weaker and the received SINR increases; therefore, MIMO provides much larger capacity than SIMO

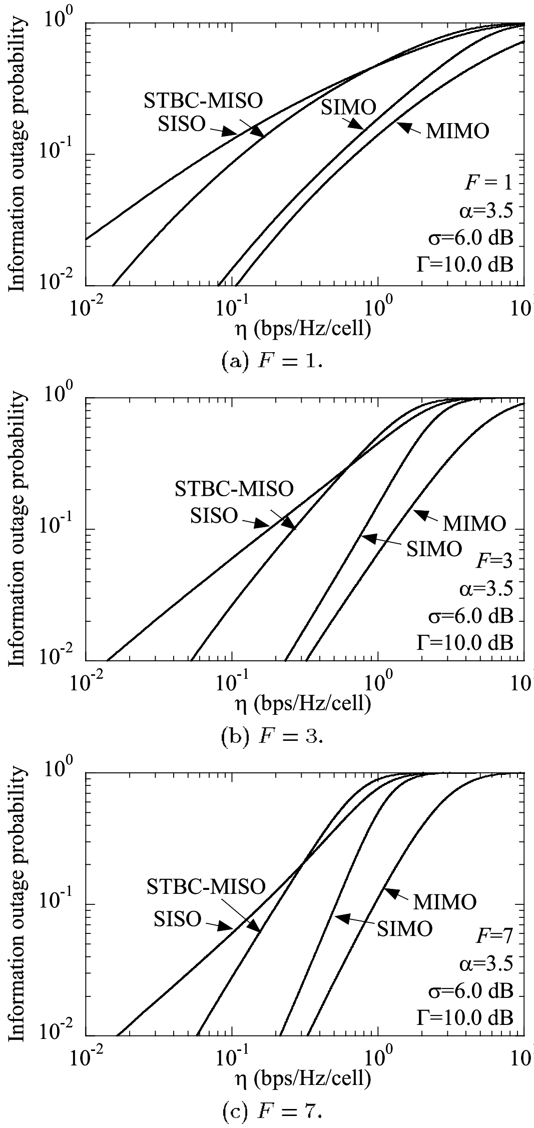

(a) $F = 1$.

(b) $F = 3$.

(c) $F = 7$.

Fig. 3 Information outage probability.

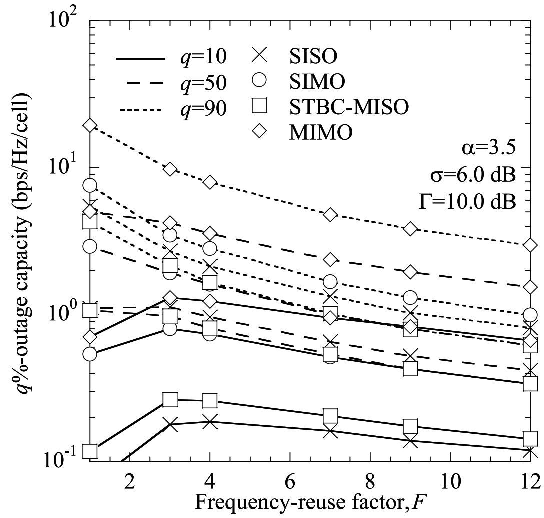

Fig. 4 Impact of frequency-reuse factor F on q%-outage capacity.

owing to the spatial multiplexing gain.

The cellular channel capacity of STBC-MISO greatly reduces compared to those of SIMO and MIMO. This is because the transmission power from each transmit antenna is reduced by a factor of N_t and because the coding rate of STBC-MISO is reduced to $3/4$ when $N_t = 3$ and 4 [7]. Therefore, the cellular channel capacity of STBC-MISO is lower than that of SIMO in spite of the same diversity order.

Bellow, we discuss the impact of frequency-reuse factor F on the cellular channel capacities of multi-antenna techniques and then, discuss about how the channel capacity is affected by propagation parameters and transmit power.

3.2 Impact of Frequency-Reuse Factor F

From the information outage probability obtained by the Monte-Carlo numerical evaluation, we find the 10%-, 50%- (median channel capacity in [4]), and 90%-outage capacities. Figure 4 plots 10%-, 50%-, and 90%-outage capacities as a function of F when the path loss exponent $\alpha = 3.5$ and the shadowing standard deviation $\sigma = 6.0$ dB.

From Fig. 4, it can be seen that if 50%-outage capacity or 90%-outage capacity is used for the system design, the use of $F = 1$ is optimal as shown in [2]–[4] and provides 50%-outage capacity of 5.0 (bps/Hz/cell) or 90%-outage capacity of 20.0 (bps/Hz/cell). On the other hand, if 10%-outage capacity is used for the system design, the use of $F = 3$ is optimal. 10%-outage capacity increases due to decreasing CCI as F increases from 1 to 3, but it decreases beyond $F = 3$. This is because the increasing total bandwidth offsets the positive effect of decreasing CCI. It can be seen from Fig. 4 that when $F = 3$, 10% of users have the cellular channel capacity below about 1.5 (bps/Hz/cell) when 4×4 MIMO is used. In other words, 90% of users enjoy the cellular channel capacity of higher than 1.5 bps/Hz/cell. Furthermore, when $F = 3$, 10% of users enjoy more than 9.0 (bps/Hz/cell). On the other hand, if a cellular system is designed using 50%-outage capacity or 90%-outage capacity, 10% of users have the cellular channel capacity lower than about 0.7 (bps/Hz/cell), although 10% of users enjoy the cellular channel capacity larger than 20.0 (bps/Hz/cell).

The above discussion shows that if the cellular system is to be designed to increase the number of users having the higher cellular channel capacity, $F = 1$ can be used; on the other hand if the system is to be designed to guarantee the minimum channel capacity, $F = 3$ can be used.

3.3 Impact of Propagation Parameters

3.3.1 Path Loss Exponent α

Figure 5 plots 10%-, 50%-, and 90%-outage capacities (bps/Hz/cell) as a function of F with the path loss exponent α as a parameter when $\sigma = 6.0$ dB.

The path loss is inverse-proportional to the α-th power

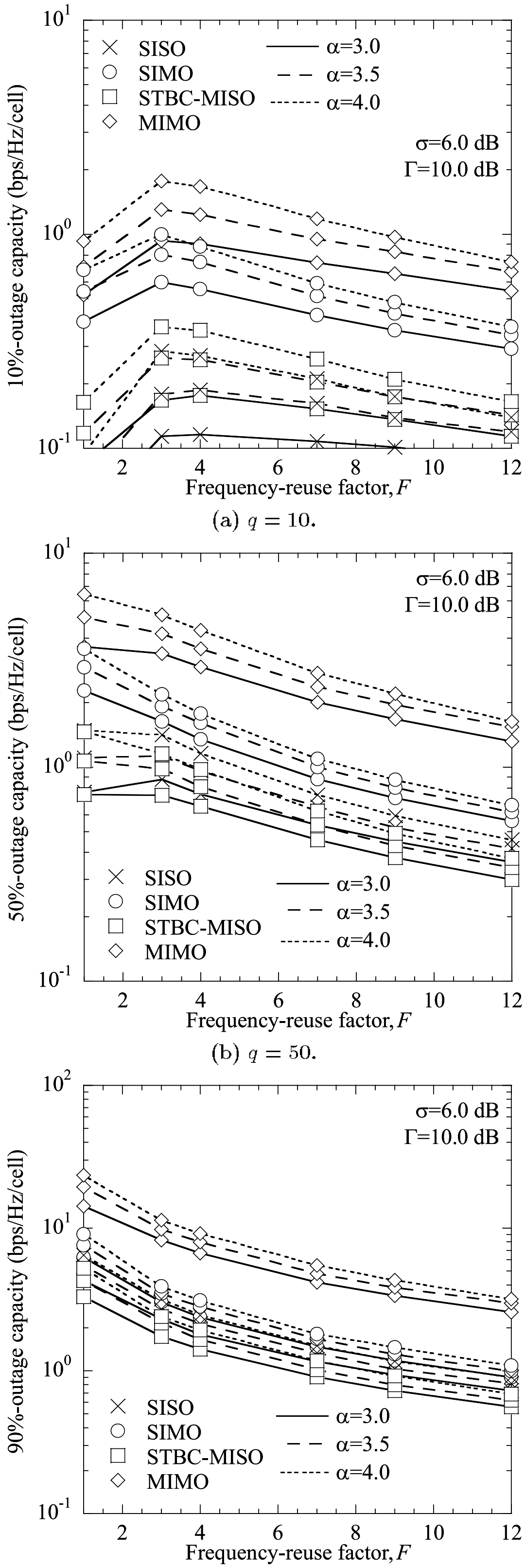

(a) $q = 10$.

(b) $q = 50$.

(c) $q = 90$.

Fig. 5 Impact of path loss exponent α on q%-outage capacity.

of the distance. The distance of an interfering BS from an MS of interest is longer than that of the desired BS. Therefore, as α increases, the CCI power attenuates much faster than the desired signal power, resulting in the increased cellular channel capacity. However, the optimum F is 3 for 10%-outage capacity irrespective of the value of α. Furthermore, it can be seen from Fig. 5 that although, 10%-, 50%-, and 90%-outage capacities increase as α increases, 90%-outage capacity is less sensitive to α compared to 10%- and 50%-outage capacities. This can be explained as follows. 90%-outage capacity is interpreted as that 10% of users in a cell have the channel capacity higher than 90%-outage capacity. These 10% users are located very close to their communicating BS and therefore, their SINR, γ is sufficiently high (since the desired signal power is high and the CCI is low). Since the channel capacity is a logarithmic function of γ as shown in Eqs. (9) and (10), the capacity variation due to the SINR variation becomes very narrow for a high SINR region. This leads to the fact that 90% outage capacity is less sensitive to α. As F increases, the impact of path loss exponent α becomes weaker irrespective of the percentage value of outage capacity. This is because, as F increases, the distance between the MS and an interfering BS increases and hence, the interference power is reduced enough even though $\alpha = 3.0$, resulting in larger γ. As a consequence, the impact of α becomes weaker when F gets larger.

3.3.2 Standard Deviation σ of Shadowing Loss

Figure 6 plots 10%-, 50%-, and 90%-outage capacities (bps/Hz/cell) as a function of F with the shadowing standard deviation σ as a parameter when $\alpha = 3.5$. As σ increases, the channel capacities reduce because the average CCI power increases due to increased variability of CCI power. Again the optimum F is seen to be 3 for 10%-outage capacity irrespective of the value of σ. Interestingly, 90%-outage capacity is almost insensitive to σ irrespective of the value of F, while 50%-outage capacity is insensitive to σ when F is larger than 7. The reason for this can be explained as follows. As discussed in 3.3.1, 90%-outage capacity is a result of contribution from the users close to their communicating BS. For such users, γ is very high and therefore, the channel capacity is insensitive to the variation of SINR and hence, σ. Similar to Sect. 3.3.1, the impact of shadowing standard deviation σ on the q%-outage capacity becomes less sensitive as F increases. This can be explained as follows. For a large F, the co-channel cells are far away from the MS of interest and hence, the CCI power is sufficiently weak. Thus, the variation of CCI power owing to shadowing has less impact on the q%-outage capacity.

3.4 Impact of Transmission Power of BS

Figure 7 plots 10%-, 50%-, and 90%-outage capacities (bps/Hz/cell) as a function of F with the received E_s/N_0 at the cell edge (i.e., transmission power of BS) as a parameter when the cell radius is kept the same for $\alpha = 3.5$ and

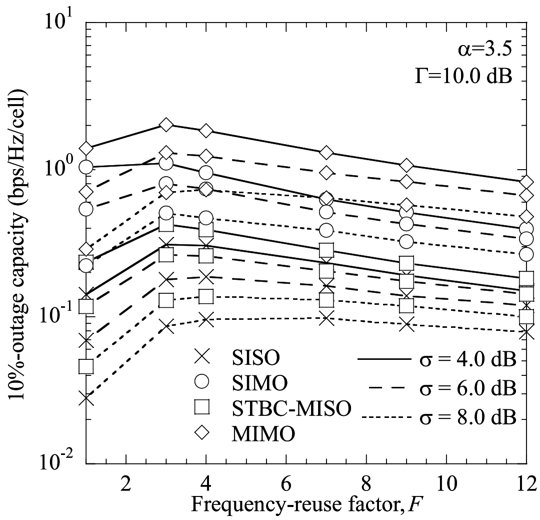

(a) $q = 10$.

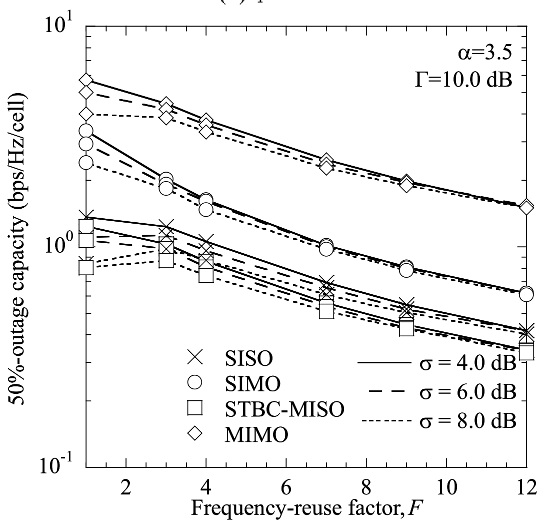

(b) $q = 50$.

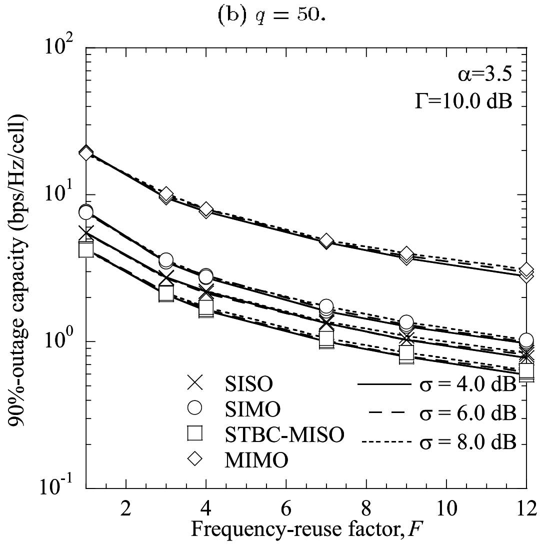

(c) $q = 90$.

Fig. 6 Impact of shadowing loss standard deviation σ on q%-outage capacity.

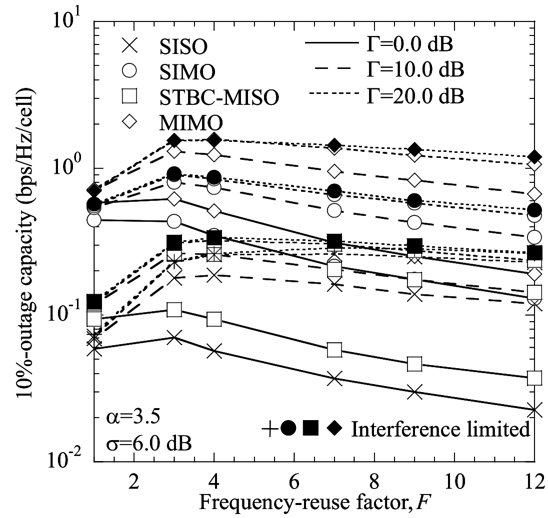

(a) $q = 10$.

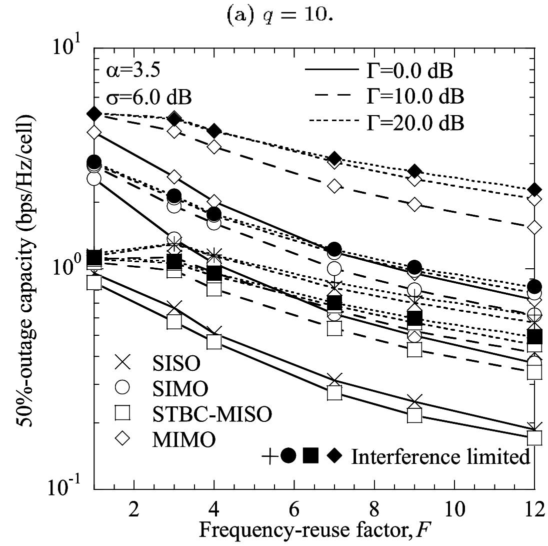

(b) $q = 50$.

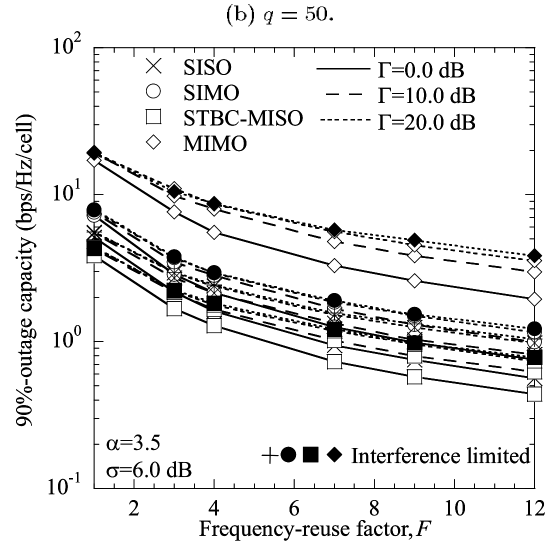

(c) $q = 90$.

Fig. 7 Impact of transmission power of BS on q%-outage capacity.

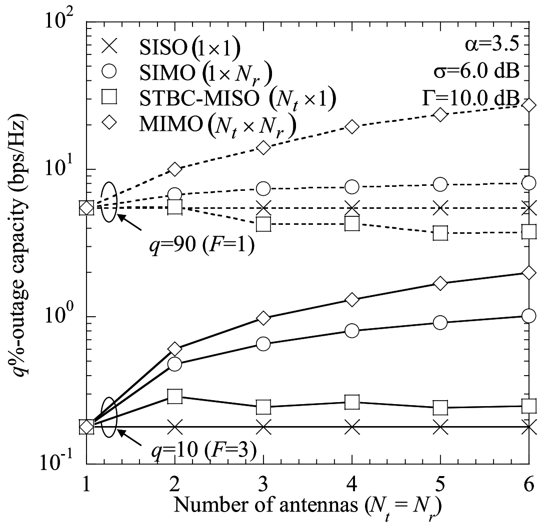

Fig. 8 Impact of the number of transmit/receive antennas on 10%- and 90%-outage capacities.

$\sigma = 6.0$ dB. For comparison, the interference-limited case (i.e., $E_s/N_0 \to \infty$) is also plotted. From Fig. 7, it can be seen that as the transmission power increases, the cellular channel capacity also increases and approaches the interference-limited case when $E_s/N_0 = 20$ dB. However, it can also be seen that the q%-outage capacity is almost insensitive to Γ irrespective of q when $F = 1$. This is because when $F = 1$, the interfering cells are near to the desired cell and the channel is almost interference-limited even if $\Gamma = 0$ dB.

3.4.1 Impact of Number of Transmit/Receive Antennas

The achievable channel capacity depends on the number of antennas. We evaluate the impact of number of transmit/receive antennas on the 10%- and 90%-outage capacities when the optimum frequency-reuse factor F is used for each outage capacity. Figure 8 plots 10%-outage capacity with $F = 3$ and 90%-outage capacity with $F = 1$ as a function of the number of transmit/receive antennas (N_t and N_r) when $\alpha = 3.5$ and $\sigma = 6.0$ dB. For comparison, the results for 1×1 SISO are also plotted. From Fig. 8, it can be seen that MIMO always provides the highest channel capacity among 1×1 SISO, $1 \times N_r$ SIMO, $N_t \times 1$ STBC-MISO and $N_t \times N_r$ MIMO. As the number of transmit/receive antennas increases, 10%- and 90%-outage capacities increase both for the MIMO and the SIMO cases. However, they are almost constant or slightly decrease for STBC-MISO case. The capacity comparison between SISO and STBC-MISO is interesting. 10%-outage capacity means that 10% of users have the channel capacity less than that. These users are far away from their communicating BS and are located close to the cell edge, therefore the received SINR is very low. In such an environment, the transmit diversity is effective to improve the SINR and the capacity of STBC-MISO is higher than that of SISO. On the other hand, 90%-outage capacity is a result of the contribution from the users near the communicating BS and the received SINR is high; therefore, the capacity is relatively insensitive to the SINR and is directly affected by the coding rate of STBC, resulting in the reduced capacity compared to SISO.

4. Conclusion

In this paper, we evaluated the information outage probability of the MIMO channel capacity from which we obtained the q%-outage capacities (which is defined as the channel capacity that gives an outage probability of q%). We compared the q%-outage capacities achievable by 1×1 SISO, 1×4 SIMO, 4×1 STBC-MISO, and 4×4 MIMO techniques and discussed the impact of propagation parameters (path loss exponent and shadowing loss standard deviation). It was shown by numerical computation that 50%- and 90%-outage capacities are almost insensitive to the propagation parameters while 10%-outage capacity is sensitive to the propagation parameters.

We have shown that the optimum reuse factor F depends on the outage probability of the channel; the optimum reuse factor F is 3 for 10%-outage capacity and the single-frequency reuse ($F = 1$) gives the largest cellular capacity for 50%- and 90%-outage capacity irrespective of path loss exponent, shadowing loss standard deviation and transmit power of BS. Furthermore, it has been shown that 4×4 MIMO can always achieve higher channel capacity than 1×1 SISO, 1×4 SIMO and 4×1 STBC-MISO.

The power allocation technique based on the water filling theory is known to enhance the capacity. The cellular channel capacity evaluation when the power allocation is used is left as an interesting future study.

References

[1] G.J. Foschini and M.J. Gans, "On limits of wireless communication in a fading environment when using multiple antennas," Wirel. Pers. Commun., vol.6, no.3, pp.311–335, March 1998.

[2] S. Catreux, P.F. Driessen, and L.J. Greenstein, "Simulation results for an interference-limited multiple-input multiple-output cellular system," IEEE Commun., Lett., vol.4, no.11, pp.334–336, Nov. 2000.

[3] S. Catreux, P.F. Driessen, and L.J. Greenstein, "Attainable throughput of an interference-limited multiple-input multiple-output (MIMO) cellular system," IEEE Trans. Commun., vol.49, no.8, pp.1307–1311, Aug. 2001.

[4] H. Huang and R.A. Valenzuela, "Fundamental simulated performance of downlink fixed wireless cellular networks with multiple antennas," Proc. IEEE 16th International Symposium on Personal, Indoor and Mobile Radio Communications 2005 (PIMRC 2005), vol.1, pp.161–165, Sept. 2005.

[5] P.J. Smith, M. Shafi, and L.M. Garth, "Performance analysis for adaptive MIMO SVD transmission in a cellular system," Proc. IEEE 7th Australian Communications Theory Workshop, pp.49–54, Feb. 2006.

[6] S.M. Alamouti, "A simple transmit diversity technique for wireless communications," IEEE J. Sel. Areas Commun., vol.16, no.8, pp.1451–1458, Oct. 1998.

[7] V. Tarokh, H. Jafarkhani, and A.R. Calderbank, "Space-time block codes from orthogonal designs," IEEE Trans. Inf. Theory, vol.45, no.5, pp.1456–1467, July 1999.

[8] L.H. Ozarow, S. Shamai, and A.D. Wyner, “Information theoretic considerations for cellular mobile radio,” IEEE Trans. Veh. Technol., vol.43, no.2, pp.359–378, May 1994.
[9] E. Biglieri, J. Proakis, and S. Shamai, “Fading channels: Information-theoretic and communications, aspects,” IEEE Trans. Inf. Theory, vol.44, no.6, pp.2619–2692, Oct. 1998.
[10] W.C. Jakes, Jr., ed., Microwave Mobile Communications, Wiley, New York, 1974.
[11] W. Su, X.G. Xia, and K.J.R. Liu, “A systematic design of high-rate complex orthogonal space-time block codes,” IEEE Commun., Lett., vol.8, no.6, pp.380–382, June 2004.
[12] P. Dent, G.E. Bottomley, and T. Croft, “Jakes fading model revisited,” Electron. Lett., vol.29, pp.1162–1163, June 1993.

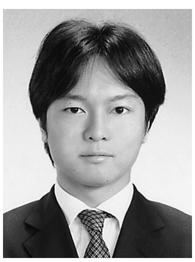

Koichi Adachi received the B.E. and M.E. degrees in Information and Science Technology from Keio University, Japan, in 2005 and 2007, respectively. Currently, he is a Japan Society for the Promotion of Science (JSPS) research fellow, and is studying toward his PhD degree at School of Science for Open and Environmental Systems, Keio University. His research interests include MIMO, channel estimation, and channel capacity. He was a recipient of the 2007 RCS (Radio Communication Systems) Active Research Award.

Fumiyuki Adachi received the B.S. and Dr.Eng. Degrees in electrical engineering from Tohoku University, Sendai, Japan, in 1973 and 1984, respectively. In April 1973, he joined the Electrical Communications Laboratories of Nippon Telegraph & Telephone Corporation (now NTT) and conducted various types of research related to digital cellular mobile communications. From July 1992 to December 1999, he was with NTT Mobile Communications Network, Inc. (now NTT DoCoMo, Inc.), where he led a research group on wideband/broadband CDMA wireless access for IMT-2000 and beyond. Since January 2000, he has been with Tohoku University, Sendai, Japan, where he is a Professor of Electrical and Communication Engineering at the Graduate School of Engineering. His research interests are in CDMA wireless access techniques, equalization, transmit/receive antenna diversity, MIMO, adaptive transmission, and channel coding, with particular application to broadband wireless communications systems. From October 1984 to September 1985, he was a United Kingdom SERC Visiting Research Fellow in the Department of Electrical Engineering and Electronics at Liverpool University. He received IEICE Fellow Award in 2007, was a co-recipient of the IEICE Transactions best paper of the year award 1996 and again 1998, and was also a recipient of Achievement award 2003. He is an IEEE Fellow and was a co-recipient of the IEEE Vehicular Technology Transactions best paper of the year award 1980 and again 1990 and also a recipient of Avant Grade award 2000. He was a recipient of Thomson Scientific Research Front Award 2004.

Masao Nakagawa was born in Tokyo, Japan in 1946. He received the B.E., M.E., and Ph.D. degrees from Keio University, Yokohama, Japan, all in electrical engineering, in 1969, 1971, and 1974 respectively. Since 1973, he has been with the Department of the Electrical Engineering, Keio University, where he is now Professor. His research interests are in CDMA, Consumer Communications, Mobile Communications, ITS (Intelligent Transport Systems). Wireless Home Networks, and Visible Optical Communication. He received 1989 IEEE Consumer Electronics Society Paper Award, 1999-Fall Best Paper Award in IEEE VTC, IEICE Achievement Award in 2000, IEICE Fellow Award in 2001, Ericsson Telecommunications Award in 2004, YRP (Yokosuka Research Park) technical Award in 2005, and IEEE Fellow Award in 2006. He is a co-author of “TDD-CDMA for Wireless Communications” published by Artech House in which the main ideas of TDD-CDMA were given by him. He was the executive committee chairman of International Symposium on Spread Spectrum Techniques and Applications in 1992 and the technical program committee chairman of ISITA (International Symposium on Information Theory and its Applications) in 1994. He is an editor of Wireless Personal Communications and was a guest editor of the special issues on “CDMA Networks I, II, III, and IV” published in IEEE JSAC in 1994 (I and II) and 1996 (III and IV). He is a chair of the Wireless Home Link sub-committee in MMAC (Multimedia Mobile Access Communication Promotion Committee).